Scientia Iranica C (2012) 19 (3), 525–534

Sharif University of Technology

Scientia Iranica

Transactions C: Chemistry and Chemical Engineering

www.sciencedirect.com

Catalytic methanation reaction over supported nickel–ruthenium oxide base for purification of simulated natural gas

W.A.W. Abu Bakar *, R. Ali, S. Toemen

Department of Chemistry, Faculty of Science, Universiti Teknologi Malaysia, 81310 UTM Skudai, Johor, Malaysia

Received 12 January 2011; revised 26 April 2011; accepted 5 November 2011

KEYWORDS

Nickel oxide;
Ruthenium oxide;
Catalyst;
Methanation;
Natural gas.

Abstract The presence of carbon dioxide and water molecules as impurities in crude natural gas decreases the quality of natural gas. Recently, the catalytic treatment of this toxic and acidic gas has become a promising technique by converting CO_2 to methane gas in the presence of H_2S gas; thus, enhancing methane production and creating an environmentally friendly approach to the purification of natural gas. A series of catalysts based on nickel oxide were prepared using the wetness impregnation technique and aging, followed by calcination at 400 °C. Pd/Ru/Ni(2 : 8 : 90)/Al_2O_3 catalyst was revealed as the most potential catalyst, and achieved 43.60% of CO_2 conversion, with 6.82% of methane formation at 200 °C. This catalyst had the highest percentage of 52.95% CO_2 conversion and yielded 39.73% methane at a maximum temperature of 400 °C. In the presence of H_2S in the gas stream, the conversion dropped to 35.03%, with 3.64% yield of methane at a reaction temperature of 400 °C. However, this catalyst achieved 100% H_2S desulfurization at 140 °C and remained constant until the reaction temperature of 300 °C. Moreover, the XRD diffractogram showed that the catalyst is highly amorphous in structure, with a BET surface area in the range of 220–270 $m^2\ g^{-1}$. FESEM analysis indicated a rough surface morphology and non-homogeneous spherical shape, with the smallest particles size in the range 40–115 nm.

1. Introduction

Nickel based catalysts are generally considered reference methanation catalysts and are known to eliminate H_2S by a desulfurization process. According to Jose et al. [1], nickel oxide exhibits high activity and selectivity for producing methane, due to the ability of NiO to undergo the reduction process owing to the presence of a defect site on the surface of NiO. It had also been reported that NiO has a bimodal pore structure, which entails high activity for CO_2 methanation [2]. This bimodal pore structure will serve as an optimum pore size for the adsorption of both reactants. The strength of adsorption on nickel has 'intermediate' binding energies for hydrogen. It also has 'intermediate' values of heat of adsorption. Souma et al. [3], showed that the methanation reaction seems to be accelerated by the absorption of H_2 on metallic nickel. Yamasaki et al. [4] found that an amorphous alloy of Ni–25Zr–5Sm catalyzed the methanation reaction, with 90% conversion of CO_2 and 100% selectivity towards CH_4 at 300 °C.

Noble metals such as rhodium, ruthenium, platinum and palladium, exhibit *s* promising CO_2/H_2 methanation performance, high stability and less sensitivity to coke deposition. Finch and Ripley [5] claimed that the noble metal promoters may enhance the activity of the catalysts to increase the conversion to methane. In addition, noble metal promoted catalysts maintained greater activity for methane conversion than non-promoted catalysts in the presence of sulfur poison. Kusmierz [6] found that ruthenium catalysts are highly selective towards methane, even if supported on Al_2O_3. The main products of the reaction were CH_4 and water. Traces of carbon monoxide were present among the product, too, but methanol was completely absent. However, Takeishi and Aika [7] who studied Raney Ru catalysts, found a small amount of methanol was produced on supported Ru catalyst, but the production of methane gas was thousands of times more than the amount of methanol from CO_2 hydrogenation.

Research done by Miyata et al. [8] revealed that the addition of Pd and Pt noble metals drastically improved the behavior

* Corresponding author. Tel.: +60 13 7466213.
E-mail address: wanazelee@yahoo.com (W.A.W. Abu Bakar).

Peer review under responsibility of Sharif University of Technology.

Production and hosting by Elsevier

1026-3098 © 2012 Sharif University of Technology. Production and hosting by Elsevier B.V. Open access under CC BY-NC-ND license.
doi:10.1016/j.scient.2012.02.004

of Ni/Mg(Al)O catalysts. The addition of noble metals on Ni resulted in a decrease in the reduction temperature of Ni and an increase in the amount of H_2 uptake on Ni on the catalyst. Panagiotopolou and Kodarides [9] found that the platinum catalyst is inactive in the temperature range of 200–400 °C, since temperatures higher than 450 °C are required in order to achieve conversion above 20%. Erdohelyi et al. [10] studied the hydrogenation of CO_2 on Rh/TiO_2. The rate of methane formation was unexpectedly higher in the $CO_2 + H_2$ reaction on Rh/TiO_2 in the presence of H_2S. At higher temperatures of 400 °C, around 75% selectivity for CH_4 formation and CO was also formed from the reaction. The selection of support is considered as important, since it may influence both the activity and selectivity of the reaction. It has also been discovered that the addition of alumina may increase methanation activity, despite the presence of low concentrations of H_2S [11]. Therefore, Al_2O_3 is selected as the support for all studied catalysts in this research.

Since the catalytic process through methanation reactions offers the best way to remove CO_2 in natural gas, the present study is to develop a catalyst based on nickel oxide by modifying the dopants using noble metals in order to fully remove this CO_2 gas at the highest conversion percentage possible at low temperatures. The addition of noble metals was studied, aiming to understand the effect of the presence of noble metals on the Ni catalyst, towards better catalytic performance.

2. Experimental

2.1. Chemicals and reagents

Nickel nitrate hexahydrate, with a chemical formula of $Ni(NO_3)_2{\cdot}6H_2O$, produced by GCE Laboratory Chemicals, was used as the base in this research. Meanwhile, ruthenium(III) chloride hydrate ($RuCl_3{\cdot}xH_2O$), palladium(II) nitrate hydrate ($Pd(NO_3)_2{\cdot}xH_2O$) and tetraamineplatinum nitrate ($(NH_3)_4Pt(NO_3)_2$), produced by Sigma Aldrich Chemical, rhodium(III) nitrate hydrate ($Rh(NO_3)_3{\cdot}xH_2O$) from Fluka Analytical, copper(II) nitrate hexahydrate ($Cu(NO_3)_2{\cdot}6H_2O$) from Riedel-de-Haën and manganese acetate tetrahydrate $Mn(CH_3COO)_2{\cdot}4H_2O$ from Rinting Scientific, were used as dopants. In addition, aluminium oxide beads (Al_2O_3) produced by MERCK Eurolab, and photocatalytic ceramic beads (SiO_2/TiO_2) produced by Titan PE Technology Inc., were used as the support materials for the preparation of catalysts. Polyethylene glycol 2000, with a chemical formula of $H(OCH_2CH_2)_nOH$ (Fluka Chemicals), and diethanolamine, with a chemical formula of $HN(CH_2CH_2OH)_2$ (Merck-Schuchardt), were used for sol–gel preparation.

2.2. Catalyst preparation

All catalysts were prepared by the aqueous incipient wetness impregnation method. The nickel loading used was 90 wt% 3 g of $Ni(NO_3)_2{\cdot}6H_20$ was dissolved in a small amount of distilled water, then mixed together with a solution of noble metal chloride salts or nitrate salts in a beaker, according to the desired ratio. A homogeneous mixture was obtained by magnetic stirring at room temperature for 30 min. For catalysts coated using a noble metal chloride precursor, the metal chloride salt was stirred in doubly distilled water and dispensed. This process was repeated several times until there were no changes occurring in the catalyst solution after $AgNO_3$ was added. This indicated that the chloride ion was completely removed. Al_2O_3 alumina beads with diameter of 4–5 mm were used as support material in this study. The support was immersed into the catalyst solution for 24 h and the supported catalysts were transferred onto an evaporating dish with glass wool on it. It was then aged inside an oven at 80–90 °C for 24 h to remove water and allow the well homogenized immobilization of the catalysts on the surface of the supported material. It was then followed by calcination in the furnace at 400 °C for 5 h, using a ramp rate of 10 °C/min, to further eliminate all metal precursors and any excess of water or impurities. A similar procedure was repeated for other ratios of the catalyst. Finally, the potential catalysts were studied in detail on various optimization parameters.

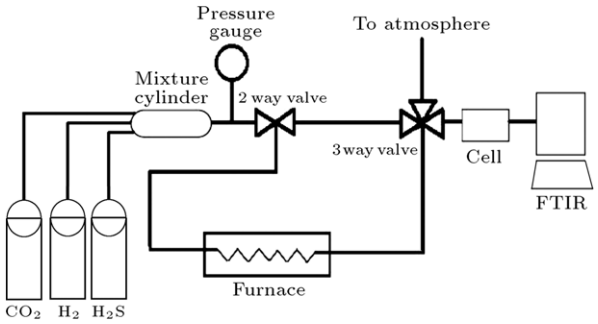

Figure 1: Schematic diagram of home-built micro reactor used for catalytic activity measurement.

2.3. Catalytic activity measurement

The supported catalyst sample was packed into a cylindrical glass tube with diameter of 10 mm and length of 360 mm, and was stored in the furnace of the home-built micro-reactor, as shown in Figure 1. No pretreatment was done prior to beginning the heating experiment. In-situ reactions of methanation and desulfurization were performed from ambient temperature up to 300 °C, with an increment temperature rate of 5 °C/min. Each experiment was repeated twice, and each treatment temperature was maintained for 30 min before the next temperature increment was accomplished. It was found that catalytic activity on the second treatment did not differ significantly. Composition of the reactant gases in comparison with the real composition of sour gases in Malaysian crude natural gas is depicted in Table 1. The mixture of CO_2 and H_2 gases was introduced into the reactor system in a stoichiometric ratio of 1:4. The product gas coming out from the furnace was collected in a FTIR sample cell and scanned at every 20 °C by a FTIR Shimadzu 8300 Spectrometer. Percentage conversion of CO_2 and H_2S was obtained by calculating the peak area of their respective stretching bands relative to the peak area of the gas during calibration without a catalyst. Off line GC analysis (Hewlett Packard 6890 Series GC System) was done to determine the yield of CH_4 gas, due to the low sensitivity of FTIR spectroscopy towards the stretching band of CH_4.

2.4. Catalyst characterization

Characterizations were studied by X-ray Diffraction (XRD), Field Emission Scanning Electron Microscope (FESEM), Nitrogen Adsorption/desorption (NA) and Thermogravimetric analysis (TGA). The XRD patterns of the prepared powder samples were recorded at 2θ between 5° and 75° using a Bruker Advance D8 with Siemens 5000 diffractometer. The Cu Kα radiation operates at 40 kV and 40 mA, with $\lambda = 1.5418$ Å.

Table 1: Flow gas mixture and chemical composition of crude natural gas from Telaga Bergading, Petronas Carigali Sdn. Bhd., analyzed by GC-MS.

Gas	Flow gas mixture (%)	Composition in crude natural gas (%)
CH_4	–	47.0
CO_2	19.0	23.5
H_2S	4.8	5.4
Others (CO, O_2, N_2)	–	24.1
H_2	76.2	–

To assess the surface by FESEM-EDX analysis, the samples were analyzed using Zeiss Supra 35 VP FESEM with the energy of 15.0 kV, coupled with the EDX analyzer and 1500× magnification. Prior to analysis, the sprinkled sample was coated with gold, as a conducting material, by gold sputter, at 10^{-1} Mbar, using the Bio Rad Polaron Division SEM coating system machine. The catalyst sample was bombarded by an electron gun, with a tungsten filament, under 25 kV resolution. The N_2 adsorption/desorption isotherm of the catalyst analyses was obtained using a Micromeritics ASAP 2010 volumetric adsorption analyzer at −196 °C. Prior to measurement, the calcined catalysts were degassed at 200 °C, overnight. The isotherms were used to determine the following parameters: surface area (using Brunauer–Emmett–Teller (BET) equation), total pore volume, total micropore volume, and total mesopore volume. TGA analysis for the samples was carried out by a TGA-SDTA 851 Mettler Toledo simultaneous thermal analyzer, up to 800 °C at 15 °C/min. The sample in the form of fine powder was placed in an alumina covered crucible, an empty crucible being the reference. Nitrogen gas, with a flow rate of 50 μL/min, was used as the atmosphere.

3. Results and discussion

3.1. Catalytic performance of supported NiO based catalyst with ruthenium as a first dopant

Table 2 illustrates the catalytic performance of supported nickel oxide based catalysts, which were calcined at 400 °C for 5 h. According to the results, a Ni/Al_2O_3 catalyst gives only 24.58% conversion of CO_2 at a reaction temperature of 400 °C. Incorporating ruthenium into this catalyst further lowered the catalytic performance towards CO_2 conversion to 7.21%. The decreasing performance of this catalyst could be due to the Ru precursor; $RuCl_3.nH_2O$ used in this study. This is in good agreement with Nurunnabi et al. [12], who found that the small amount of chloride ion in the Ru/Al_2O_3 catalyst could lead to a decrease in the active sites of the Ru catalyst surface. The presence of residual chloride ions forms a partition between the support and the metal, and therefore inhibits both CO and hydrogen chemisorption phenomena on the catalyst surface [12].

However, the addition of palladium into the $Ru/Ni(10:90)/Al_2O_3$ catalyst to form $Pd/Ru/Ni\ (2:8:90)/Al_2O_3$ catalyst coincidentally enhanced catalytic activity for the conversion of CO_2 of the prepared catalysts. It showed 37.94%, 43.60% and 45.77% of CO_2 conversion at reaction temperatures of 100 °C, 200 °C and 300 °C, respectively, while 52.95% CO_2 conversion was achieved at the maximum studied temperature of 400 °C. This suggests that small amounts of Pd addition can play an important role in the improvement of catalyst activity. This is in accordance with the findings of Baylet et al. [13] who studied the catalytic activity and stability of Pd doped hexaaluminate catalysts for the CH_4 catalytic combustion. They found that the addition of palladium to the alumina support material gives a sufficient absorption for the CO_2 dissociation process, which is due to the increasing of active sites created on the catalyst surface.

Table 2: Percentage conversion of CO_2 from methanation reaction over various alumina supported nickel oxide based catalysts with ruthenium as a dopant and co-dopant.

Alumina supported catalysts	Reaction temperature			
	100 °C	200 °C	300 °C	400 °C
	% conversion of CO_2			
$Ni\ (100\%)/Al_2O_3$	6.35	10.86	18.15	24.58
$Ru/Ni\ (10:90)/Al_2O_3$	1.26	1.89	3.94	7.21
$Pd/Ru/Ni\ (2:8:90)/Al_2O_3$	**37.94**	**43.60**	**45.77**	**52.95**
$Pt/Ru/Ni\ (2:8:90)/Al_2O_3$	10.75	18.03	32.33	34.74
$Rh/Ru/Ni\ (2:8:90)/Al_2O_3$	3.23	5.67	11.00	19.29
$Ru/Mn/Ni\ (2:8:90)/Al_2O_3$	7.74	22.19	26.31	34.86
$Ru/Cu/Ni\ (2:8:90)/Al_2O_3$	14.62	24.02	24.88	25.87
$Ru/Pd/Ni\ (2:8:90)/Al_2O_3$	17.30	22.58	28.77	35.64

When platinum was added into the Ru/Ni catalyst, the $Pt/Ru/Ni\ (2{:}8{:}90)/Al_2O_3$ catalyst did not perform well, and managed to convert only 34.74% at the maximum reaction temperature, 400 °C, while at 200 °C, the conversion of CO_2 was around 18.03%. Bi et al. [14] reported that the Pt catalyst is generally effective for the Reverse Water–Gas Shift (RWGS) reaction. It can be seen from Table 2 that the result of Ru/Ni doped with Pt was not as good as Ru/Ni doped with Pd. It showed that Pd is better than Pt. Our finding was in agreement with Lapisardi et al. [15] who revealed that the conversion rate of the Pd catalyst was four times higher than that of the Pt catalyst for the production of syngas. As previously reported by Gelin et al. [16], Pd/Al_2O_3 did not exhibit any deactivation with time, on stream, under experimental conditions, but Pt/Al_2O_3 slowly deactivates with time. The decreasing activity of this catalyst is mostly due to the sintering of Pt particles, exaggerated by local hot spots, owing to the highly exothermic CO_2 methanation reaction, which is responsible for the loss of Pt dispersion [17].

The presence of rhodium in the $Rh/Ru/Ni\ (2:8:90)/Al_2O_3$ catalyst was even worse, with poor activity and selectivity in comparison to Ni/Al_2O_3. Only 19.29% CO_2 conversion was observed under similar experimental conditions, even at the highest reaction temperature of 400 °C. These findings might be explained by the fact that the addition of Rh in this catalyst caused poor metal dispersion. This was also reported by Wachs [18], and the reason given was due to the poor interaction between active basic metal oxide and the support material. Thus, the metals are easily migrated and sintered to form large metal particles [19], leading to the agglomeration on the surface of the catalyst, which will reduce the degree of dispersion. Furthermore, when Ru was added into the $Mn/Ni/Al_2O_3$ catalyst to form the $Ru/Mn/Ni\ (2:8:90)/Al_2O_3$ catalyst, it did not show good performance in its catalytic activity, which only gave 22.19% and 34.86% of CO_2 conversion at reaction temperatures of 200 °C and 400 °C, respectively. Meanwhile, the CO_2 conversion of $Ru/Cu/Ni/Al_2O_3$ catalyst with a ratio of 2:8:90 gave no more than 25.87% of conversion, even at the maximum reaction temperature of 400 °C.

Pd and Ru are a good combination for Ni based catalysts only when the ratio of Ru is higher than that of Pd. It can be observed from Table 2 that only 35.64% of CO_2 conversion was obtained at the reaction temperature of 400 °C for the $Ru/Pd/Ni\ (2:8:90)/Al_2O_3$ catalyst compared to the $Pd/Ru/Ni\ (2:8:90)/Al_2O_3$ catalyst. From the results, it was suggested that the

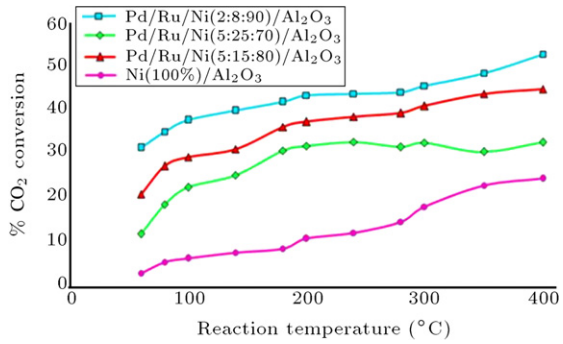

Figure 2: Catalytic performance of CO_2 conversion from methanation reaction over Pd/Ru/Ni/Al_2O_3 catalyst calcined at 400 °C for 5 h with various loading of nickel: (i) 90 wt% (Pd/Ru/Ni (2 : 8 : 90)/Al_2O_3), (ii) 80 wt% (Pd/Ru/Ni (5 : 15 : 80)/Al_2O_3) and (iii) 70 wt% (Pd/Ru/Ni (5 : 25 : 70)/Al_2O_3).

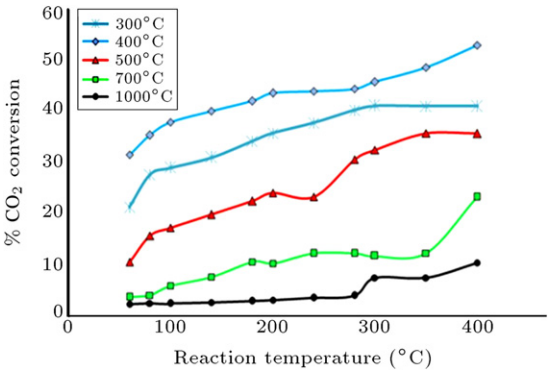

Figure 3: Catalytic performance of CO_2 conversion from methanation reaction over Pd/Ru/Ni (2:8:90)/Al_2O_3 catalyst calcined for 5 h at different calcination temperatures: (i) 400 °C, (ii) 500 °C, (iii) 700 °C, (iv) 1000 °C, and (v) 300 °C.

Pd/Ru/Ni (2 : 8 : 90)/Al_2O_3 catalyst is the potential catalyst for CO_2 conversion. Generally, the conversion rate of CO_2 for all prepared catalysts increased with the increasing of reaction temperature.

Based on the results taken from catalytic activity testing, it was found that Pd/Ru/Ni (2 : 8 : 90)/Al_2O_3 was the potential catalyst for CO_2 conversion. Several optimization parameters were conducted on these catalysts including the amount of Ni loading, the calcination temperature of the supported catalyst, the type of support material, method of preparation, H_2S testing, reproducibility testing and, finally, regeneration testing.

3.1.1. Effect of nickel loading

Figure 2 compares the amount of Ni loading towards the percentage CO_2 conversion by the Pd/Ru/Ni/Al_2O_3 catalyst. The Ni loadings used were 90, 80 and 70 wt%. The catalytic activity of the Pd/Ru/Ni (5:25:70)/Al_2O_3 catalyst is only slightly lower than that observed on the same catalyst, with Ni loadings of 90 and 80 wt%. The CO_2 conversions over the Pd/Ru/Ni(5:25:70)/Al_2O_3 catalyst reached their maximum conversions at 400 °C, around 32%, and achieved 45.06% for the Pd/Ru/Ni (5:15:80)/Al_2O_3 catalyst at the same reaction temperature. The lowest activity of the Ni catalyst, with the lowest amount of Ni, was due to partial Ni particles located in the pores, thus, leading to lesser active sites for the reduction process, as mentioned by Perkas et al. [20]. From this observation, it can be concluded that the catalytic activity of Ni loading follows a trend in the order of 90 wt% > 80 wt% > 70 wt%. The selection of metal loading is tremendously important in order to properly balance the activity with selectivity. Then, these catalysts were further analyzed by varying the calcination temperature of the supported catalyst.

3.1.2. Effect of different calcination temperature towards supported catalyst

This parameter was investigated to determine the effect of calcination temperature on alumina supported catalyst towards CO_2 conversion. Pd/Ru/Ni (2:8:90)/Al_2O_3 catalyst was coated on alumina and aged in an oven for 24 h before calcined the catalyst at five different temperatures of 300, 400, 500, 700 and 1000 °C. Figure 3 indicates the trend plot of catalytic activity over Pd/Ru/Ni (2:8:90)/Al_2O_3 at various calcination temperatures.

From Figure 3, it can be observed that the highest CO_2 conversion was obtained from the Pd/Ru/Ni (2:8:90)/Al_2O_3 catalyst calcined at 400 °C, with 43.60% conversion, followed by the Pd/Ru/Ni (2:8:90)/Al_2O_3 catalyst calcined at 500 and 700 °C, which achieved only 24.1% and 10.36% of CO_2 conversion at 200 °C, respectively. This phenomena could be explained by the drastic increase in calcination temperature, which decreases the specific surface area of the solids and, thus, catalytic activity. This is probably due to the deep encapsulation of sintered noble metal particles, which limit its diffusion by reducing the pore size, as stated in the research of Ruckenstein and Hu [21]. As expected, further increase of calcination temperature to 1000 °C induces the decreasing of catalytic activity over this Pd/Ru/Ni (2:8:90)/Al_2O_3 catalyst. However, the Pd/Ru/Ni (2:8:90)/Al_2O_3 catalyst calcined at 300 °C achieved 35.77% CO_2 conversion at a reaction temperature of 200 °C. It can be concluded in this research that 400 °C was the optimum calcination temperature over the Pd/Ru/Ni (2:8:90)/Al_2O_3 catalyst. In other words, the conversion of CO_2 over the alumina supported catalyst in this research, with different calcination temperatures, is in the following increasing order: 400 °C > 300 °C > 500 °C > 700 °C. It was then further optimized by varying the support materials.

3.1.3. Effect of different support materials

As the acid or base properties of the support may influence the catalysts, either electronically or structurally, the potential Pd/Ru/Ni (2:8:90) catalyst calcined at 400 °C was chosen to be supported on various supports, such as alumina beads (Al_2O_3), TiO_2/SiO_2 beads and carbon chips from the palm kernel shell in order to compare the compatibility and suitability of the supports towards the catalyst. The comparison of the support effect towards the catalytic performance of the Pd/Ru/Ni (2:8:90) catalyst is summarized in Figure 4.

It could be seen that catalysts on the Al_2O_3 support gave the highest CO_2 conversion. It still appeared as the most suitable support, as it showed a stable performance on CO_2 conversion. The carbon support from the palm kernel shell was found to convert 25.54% of CO_2 at the reaction temperature of 200 °C. Meanwhile, theTiO_2/SiO_2 support gives a very low conversion of CO_2 (4.8%) at 200 °C, and achieved a maximum CO_2 conversion of 17.87% at the maximum studied reaction temperature of 400 °C. These results implied that the TiO_2/SiO_2 support was not appropriate for CO_2 conversion, as also suggested by Takenaka et al. [22]. They found that TiO_2/SiO_2 supported catalysts are effective for the complete removal of CO through methanation, because they react more strongly with the metal surface compared to CO_2. De Boer et al. [23] reported that less than

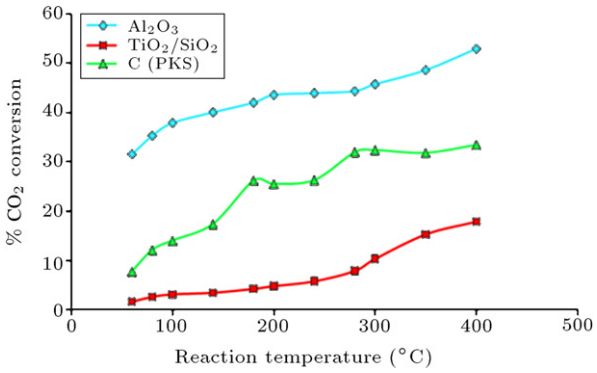

Figure 4: Catalytic performance of CO_2 conversion from methanation reaction over Pd/Ru/Ni (2:8:90) catalyst with various support materials: (i) Al_2O_3 beads (ii) TiO_2/SiO_2 beads and (iii) Carbon chips from PKS calcined at 400 °C for 5 h.

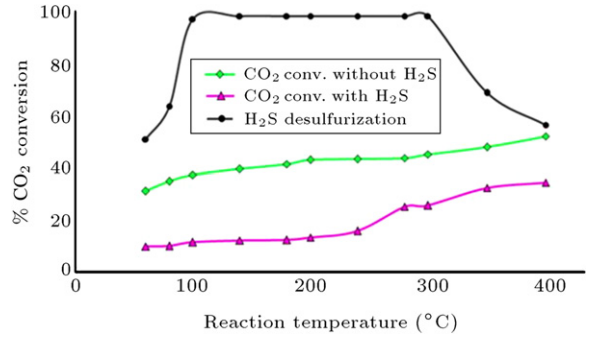

Figure 5: Catalytic performance of CO_2 conversion from methanation reaction over Pd/Ru/Ni (2:8:90)/Al_2O_3 catalyst calcined at 400 °C for 5 h testing with and without the presence of H_2S gas.

100% metal oxide dispersion on the SiO_2 support was obtained, because of lower reactivity and the higher acidic character of this support. Such properties will decrease its reduction ability of CO_2 to CH_4 during catalytic testing. In other words, the conversion of CO_2 over Pd/Ru/Ni (2:8:90), with different support, is in the following increasing order: Pd/Ru/Ni (2:8:90)/Al_2O_3 > Pd/Ru/Ni (2:8:90)/Carbon > Pd/Ru/Ni (2:8:90)/TiO_2. Further, the catalyst was undergoing other optimization parameters, which are calcination temperatures of the alumina support.

3.1.4. *Effect of* H_2S *gas on the alumina supported catalysts*

The potential catalysts were further tested for the CO_2 methanation reaction in the presence of H_2S to check the durability of the catalysts. In the presence of a sulfur compound in the gas stream, nickel catalysts for CO_2 methanation are easily deactivated. Thus, the toughness of the catalyst towards the H_2S attack is an important factor for the practical use of catalysts, as has been suggested by Habazaki et al. [24]. Figure 5 indicates the comparison of catalytic activity over the Pd/Ru/Ni (2:8:90)/Al_2O_3 catalyst in the presence of H_2S gas.

As seen in the above figure, the Pd/Ru/Ni (2:8:90)/Al_2O_3 catalyst had achieved 100% H_2S desulfurization at 100 °C, to sulfur, and remains constant until the reaction temperature of 300 °C. It began to decrease from 100% to 57.31% at temperatures 300–400 °C. The catalyst lost its H_2S activity, probably due to the high concentration of S, which forms an external layer on the catalyst surface, preventing the next incoming H_2S from passing and continuing its reaction with active sites of the catalyst, as suggested by Hassan [25].

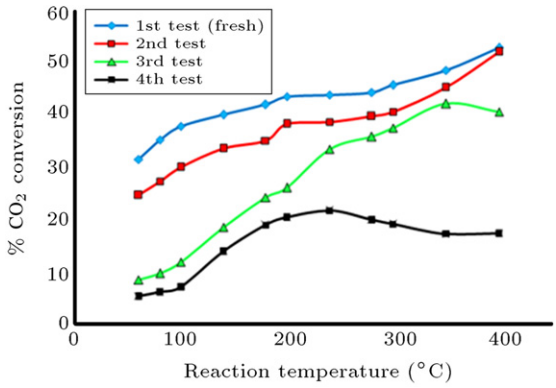

Figure 6: The trend plot of reproducibility testing over Pd/Ru/Ni (2:8:90)/Al_2O_3 catalyst calcined at 400 °C for 5 h towards CO_2 conversion from methanation reaction.

It seems that in the presence of H_2S, the conversion of CO_2 decreased to around 30.07% of its performance, from 43.6% to 13.53% at 200 °C, indicating that the catalyst was poisoned by the sulfur compound. This sulfur compound is more active in making an interaction between the catalysts, blocking the pore on the surface of the catalyst and, hence, retarding the reduction of CO_2 during the reaction. This is in a good agreement with results reported previously, that the adsorption of H_2S on Ni is very strong, which, then, deactivates the nickel based samples by chemisorption on the metal catalyst [10,26].

3.1.5. *Reproducibility testing towards potential catalyst*

The reproducibility catalytic activity of the catalyst was tested using the same catalyst several times until the catalyst was deactivated. Figure 6 shows the trend plot of reproducibility testing over the Pd/Ru/Ni (2:8:90)/Al_2O_3 catalyst. It can be seen that the conversion of CO_2 over the fresh catalyst is 43.60% at the reaction temperature of 200 °C. However, the conversion was slightly decreased to 35.10% after the second testing, using the spent catalyst, and continuously decreased to 26.17% for the third testing over the same spent catalyst at the same reaction temperature. For the fourth testing, CO_2 conversion was lower, even though the conversion of the catalyst kept increasing from temperatures of 60–240 °C, and then slowly deactivating until the maximum studied temperature of 400 °C. From the observation in Figure 6, it can be suggested that the Pd/Ru/Ni (2:8:90)/Al_2O_3 catalyst started to deactivate after the first testing.

3.1.6. *Regeneration testing on the potential catalyst*

This experiment was demonstrated to determine the optimum operating conditions needed to regenerate the spent catalyst and re-test its activity. The spent catalyst from Section 3.1.5 was used to carry out this experiment. Figure 7 shows the trend of the regenerated catalyst testing of the Pd/Ru/Ni (2:8:90)/Al_2O_3 catalyst at various temperatures and times. There are two methods of catalyst regeneration process: oxidative regeneration and non-oxidative regeneration as classified by Furimsky and Massoth [27]. In this research, the regeneration process is categorized as oxidative regeneration, because the waste catalyst was exposed to the oxygen. Eq. (1) seems to include the idea of using compressed air in this research:

$$NiC_{(p)} + 3O_{2(g)} \underset{\Delta}{\rightarrow} 2NiO_{(p)} + 2CO_{2(g)}. \quad (1)$$

Table 3: The product and by-product of CO_2 methanation reaction over Pd/Ru/Ni (2:8:90)/Al_2O_3 catalyst detected via GC.

Catalyst	Reactant	Reaction temp (°C)	CO_2 conversion (%)		Selectivity (%)	Unreacted CO_2 (%)
			Product CH_4	By-product $CO + H_2O$		
Pd/Ru/Ni (2:8:90)/Al_2O_3	CO_2	100	2.78	35.16	7.33	62.06
		200	6.82	36.78	15.64	56.40
		300	15.95	29.82	34.85	54.23
		400	39.73	13.22	75.03	47.05
	$CO_2 + H_2S$	100	0.35	11.19	3.03	88.46
		200	1.73	11.80	12.79	86.47
		300	2.61	23.36	10.05	74.03
		400	3.64	31.39	10.39	64.97

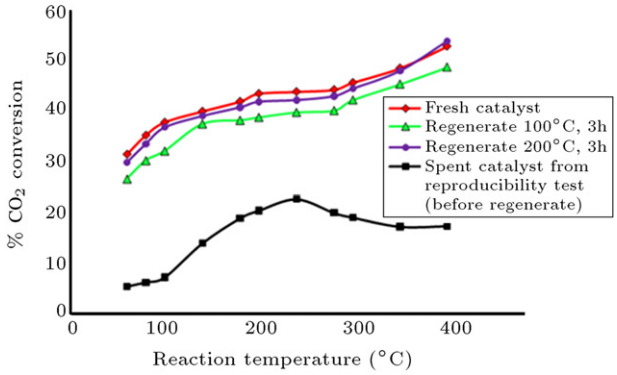

Figure 7: Regeneration catalytic testing over Pd/Ru/Ni (2:8:90)/Al_2O_3 catalyst for 3 h at various temperatures towards CO_2 conversion from methanation reaction.

The use of compressed air in this research is the most practical approach, since the industrial equipment used for the regeneration temperature is usually limited to 430 °C, as suggested by Trimm [28]. Figure 7 reveals that the carbon was removed from the Pd/Ru/Ni (2:8:90)/Al_2O_3 catalyst surface by heating the catalyst at 200 °C for 3 h in the flow of compressed air, since the conversion of CO_2 was comparable to that fresh catalyst, which was 42%. Therefore, the Pd/Ru/Ni (2:8:90)/Al_2O_3 catalyst can be reused without losing its good catalytic activity.

3.2. Methane gas formation measurement via gas chromatography

The reactor gas product from the FTIR cell was collected and analyzed for CH_4 formation. The methane formation was determined via GC, because of the low sensitivity of FTIR spectroscopy towards the methane stretching region. Table 3 shows the testing results of CO_2/H_2 methanation over the potential alumina supported catalyst. There are three possible products obtained during the CO_2 methanation reaction, namely, carbon monoxide, water and methane. From Table 3, it can be seen that the percentage of unreacted CO_2 decreases as the CO_2 was converted into CH_4, CO and H_2O, while the CH_4 content increased as the temperature increased. However, the CO_2 methanation in this research could be considered a partial oxidation reaction. This is because the formation of CO and the amount of unreacted CO_2 are higher than the formation of CH_4.

Even at the reaction temperature of 200 °C, the conversion of CO_2 did not yield 100% CH_4, but tended to form CO and H_2O. These results are in good agreement with other researchers. Yaccato et al. [17] found that when the methanation process was tested, the main product observed was CO at low temperature and, when using higher temperature, CH_4 was formed. This is due to the indirect conversion of CO_2 into C_1 hydrocarbons through the formation of intermediate CO, as suggested by Silver et al. [29]. Only 39.73% of methane was formed over this catalyst at the maximum studied temperature.

The methane production lowered when the CO_2 methanation was conducted in the presence of H_2S over the Pd/Ru/Ni (2:8:90)/Al_2O_3 catalyst. At 200 °C, the methane production decreased from 6.82% to 1.73%, while at 400 °C, the formation of methane dropped around 91% from 39.73% to only 3.64% indicating that the catalyst was possibly poisoned by the presence of H_2S in the gas stream. The active sites of the catalyst were blocked by the sulfur compound. This phenomenon prevents CO_2 and H_2 from being absorbed and converted to CH_4 on the surface of the catalyst.

3.3. Characterization of the potential catalysts

3.3.1. X-ray diffraction analysis (XRD)

Figure 8 shows the diffractograms of XRD analysis for the Pd/Ru/Ni (2:8:90)/Al_2O_3 catalysts, which were calcined at 400, 700 and 1000 °C. The XRD diffractogram for the potential catalyst that was calcined at 400 °C showed a very low degree of crystallinity and a high noise to signal ratio. It can be seen that the slight significant peaks in the diffractogram could all be attributed to the presence of Al_2O_3, as the support for the catalyst which occurred centered at $2\theta = 67.000°$ and 37.000°. Research done by Wang et al. [30] also reveals that no crystalline phases were detected in the Cu–Mn–O/Al_2O_3 catalyst that was calcined at 400 °C by XRD, because the active components of metal oxides are highly dispersed in the alumina support, which is highly amorphous.

However, at a calcination temperature of 700 °C, the intensity of alumina peaks over the Pd/Ru/Ni (2:8:90)/Al_2O_3 catalyst was slightly increased and became more profound. This revealed that an intermediate crystallinity was observed in this catalyst. The phase that was dominated by alumina support was revealed as cubic Al_2O_3 at $2\theta = 67.114$ (I_{100}), 45.450 (I_{100}), and 37.505° (I_{90}) with d spacing value of 1.393, 1.994 and 2.396 Å (PDF d values for cubic Al_2O_3 (Å) = 1.403, 1.985 and 2.394 Å). From the calculation based on the relative intensity ratio, the overlapping of cubic NiO diffraction peaks with those of the support peaks was assumed to be occurred at 2θ of 45.450° (I_{100}) and 37.505 (I_{68}), with d spacing values of 1.994 and 2.396 Å (PDF d values for cubic NiO (Å) = 2.088 and 2.412 Å).

Interestingly, four new peaks were also observed in the XRD pattern. Among the four peaks, one peak was obtained as cubic NiO at 2θ of 62.878° (I_{44}), with d spacing value of 1.463 Å (PDF

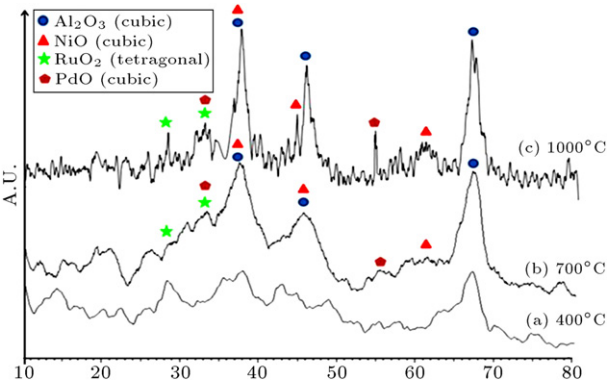

Figure 8: XRD diffractograms of Pd/Ru/Ni (2:8:90)/Al_2O_3 catalyst calcined at (a) 400 °C, (b) 700 °C and (c) 1000 °C for 5 h.

d values for NiO (Å) = 1.477 Å). The other two peaks were obtained at 2θ of 28.198 (I_{100}) and 34.066° (I_{77}), with d spacing values of 3.162 and 2.630 Å (PDF d values for RuO_2 (Å) = 3.182 and 2.690 Å), and were assigned for the tetragonal of RuO_2. As shown by Graph (b) in Figure 8, the pattern showed very small peaks, which were hardly distinguishable from the background noise, possibly indicating that there was only a very small amount of RuO_2 present on the surface, or that the particles dispersed on the support were relatively small. A similar species of the tetragonal RuO_2 phase was also observed by Chen et al. [31] at diffraction peaks of 2θ = 28.000°, and 35.100° over the Ru–La_2O_3/Al_2O_3 catalyst, even calcination at a temperature of 500 °C. It can be suggested that the presence of RuO_2 is not resolved over the catalyst.

The cubic phase of PdO peaks was assumed in the envelope of RuO peaks at 2θ of 34.066° (I_{100}) or d spacing values of 2.630 Å (PDF d value for PdO (Å) = 2.820 Å). Meanwhile, the emergence of a new broad peak at 2θ of 54.177° (I_{70}), with d spacing value of 1.692 (PDF d value for PdO (Å) = 1.630 Å), was also observed for the same compound.

All peaks observed became more intense, sharper and narrower when the catalyst was calcined at 1000 °C (Graph (c) in Figure 8) indicating that the degree of crystanallity over the Pd/Ru/Ni (2:8:90)/Al_2O_3 catalyst increased with increasing calcination temperature. The highest intensity was also due to the cubic phase of Al_2O_3 at 2θ = 66.671 (I_{100}), 45.648° (I_{100}) and 37.416 (I_{90}) or d spacing values of 1.402, 1.986 and 2.402 Å (PDF d values for cubic Al_2O_3 (Å) = 1.403, 1.985 and 2.394 Å).

In addition, one of the peak corresponding to the cubic NiO was covered with alumina support at 2θ of 37.416 (I_{68}) or d spacing values of 2.402 Å (PDF d values for cubic NiO(Å) = 2.412 Å). Another two peaks appeared sharply at 2θ of 43.294 (I_{100}) and 62.902° (I_{44}) or d spacing values of 2.088 and 1.476 Å (PDF d values for cubic NiO (Å) = 2.088 and 1.477 Å). The nickel oxide cubic phase is thermostable and it can prevent the changing phase from occurring, as suggested by Richardson et al. [32].

Furthermore, peaks assigned to the tetragonal of RuO remained similar at 2θ of 27.265° (I_{100}) and 32.131 (I_{77}) or d spacing values of 3.268 and 2.783 Å (PDF d values for RuO_2 (Å) = 3.182 and 2.690 Å). In the meantime, the broad peaks of the PdO cubic phase have been transformed into high intensity and sharper peaks at 2θ of 31.702 (I_{100}) and 56.820° (I_{90}) or d spacing values of 2.820 and 1.619 Å (PDF d values for PdO (Å) = 2.820 and 1.630 Å).

However, all the NiO, RuO_2 and PdO species were not observed in the catalyst that was calcined at 400 °C (Graph (a) in Figure 8). It can be suggested that these species are present with small crystallite size and highly dispersed, so, they could not be detected, due to the insensitivity of the XRD instrument. This was confirmed by EDX analysis, which showed the existence of Ni, Ru, Pd, Al and O elements in the Pd/Ru/Ni (2:8:90)/Al_2O_3 catalyst itself. Therefore, it can be concluded that these species can lead to a higher conversion of CO_2 at a reaction temperature of 200 °C, as shown in Figure 3. The highest CO_2 conversion was obtained for the Pd/Ru/Ni (2:8:90)/Al_2O_3 catalyst calcined at 400 °C (43.60%), followed by the Pd/Ru/Ni (2:8:90)/Al_2O_3 catalyst calcined at 500 °C (24.10%), 700 °C (10.36%) and 1000 °C (3.16%). The formation of active species, such as the cubic phase of NiO, also leads to higher catalytic activity towards the CO_2 methanation reaction.

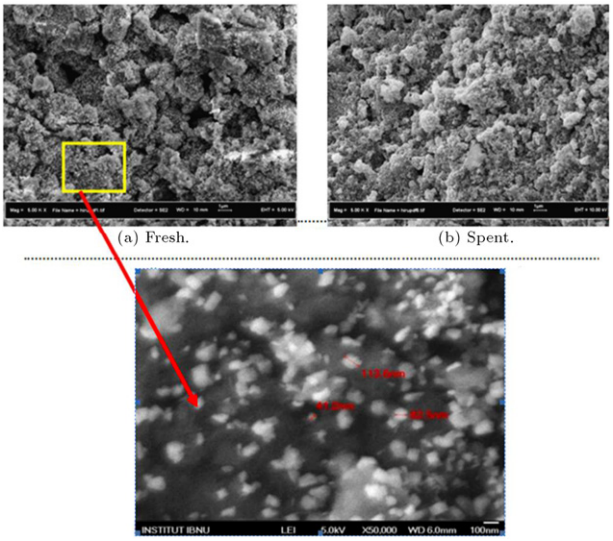

Figure 9: FESEM micrographs of fresh and spent Pd/Ru/Ni (2:8:90)/Al_2O_3 catalysts, calcined at 400 °C for 5 h with magnification 5000× and 50,000×.

3.3.2. Field emission scanning electron microscopy and energy dispersive X-ray

Figure 9 shows the FESEM micrographs of fresh and spent Pd/Ru/Ni (2:8:90)/Al_2O_3 catalysts, calcined at 400 °C for 5 h with magnification of 5000× and 50,000×. The fresh Pd/Ru/Ni (2:8:90)/Al_2O_3 catalyst showed rough surface morphology with an inhomogeneous spherical shape, and comes with small particles sizes. The morphology of the fresh catalyst changed significantly after the hydrogenation of the methanation reaction, which showed the formation of aggregated and agglomerated undefined shapes on the surface of the spent catalyst (Figure 9(b)). This observation was possibly due to the heat generated during the catalytic reaction, which caused the catalyst to agglomerate, thus, decreasing the activity, as shown in Figure 6.

In this research, it was found that the particle size of fresh Pd/Ru/Ni (2:8:90)/Al_2O_3 catalyst is categorized at the nano (<100 nm) level, which varies from 40 to 115 nm. The smaller particle size plays an important role in exhibiting higher catalytic activity. This result is consistent with the results of the XRD analysis, which revealed very broad peaks, denoting the amorphous state observed in the diffractogram calcined at 400 °C, caused by the very small nanocrystallite sizes. The smaller particle size of the catalyst will lead to the higher dispersion of the catalyst and the large surface area of the

Table 4: EDX analysis of fresh and spent Pd/Ru/Ni (2:8:90)/Al_2O_3 catalysts calcined at 400 °C for 5 h.

Catalyst	Weight ratio (%)					
	Al	O	Ni	Ru	Pd	C
Fresh catalyst	38.46	50.69	3.33	4.64	2.89	–
Spent catalyst	36.33	44.58	4.33	7.77	3.19	3.80

Table 5: BET surface area and average pore diameter of the fresh and spent Pd/Ru/Ni (2:8:90)/Al_2O_3 catalyst calcined at 400 °C for 5 h.

Catalyst	Condition	S_{Bet} (m^2g^{-1})	Average pore diameter (Å)
Pd/Ru/Ni (2:8:90)/Al_2O_3	Fresh	266.10	50.3841
	Spent	221.97	58.3265

supported nickel oxide based catalyst. One of the most efficient ways to improve the reactivity for CO_2 methanation is to use materials with a large surface area and high dispersion, as explained by Kodama et al. [33].

Furthermore, Table 4 shows the EDX analysis for the fresh and spent Pd/Ru/Ni (2:8:90)/Al_2O_3 catalysts. The elemental analysis performed by EDX confirmed the presence of Ni, Ru, Pd, Al and O in the potential catalyst.

From EDX analysis, it can be observed that the composition of Ru was higher than the composition of Ni on the fresh and spent Pd/Ru/Ni (2:8:90)/Al_2O_3 catalysts. This phenomenon can be explained, due to the incorporation of Ni into the support after calcination of the respected catalyst at 400 °C. This is in good agreement with the findings observed by Nurunnabi et al. [12], who claimed that Ni may have been adsorbed into the porous support, hence, the lower concentration of Ni on the catalyst surface than can be detected by EDX. The migration of Ni atoms from bulk matrices to the surface of the catalyst making the higher composition of Ni was detected for the spent catalyst.

Moreover, the spent Pd/Ru/Ni (2:8:90)/Al_2O_3 catalyst confirms the existence of 3.80% carbon on the surface of the catalyst. The difference of fresh and spent catalyst surfaces was due to the presence of carbon, as shown in FESEM analysis (Figure 9). The formation of agglomerated catalyst particles in the spent Pd/Ru/Ni (2:8:90)/Al_2O_3 catalyst was observed. As mentioned by Hu and Lu [34], the catalyst containing nickel is subjected to deactivation by carbon after running the catalytic testing. The low activation energy also can be related to deactivation by coke formation at higher temperature, as explained by Paál et al. [35]. However, the surface state under these conditions is regenerable as confirmed by the regeneration reaction on this catalyst, as discussed in Section 3.1.6.

3.3.3. Nitrogen absorption analysis (NA)

The potential catalysts, Pd/Ru/Ni (2:8:90)/Al_2O_3, in fresh and spent forms, were characterized by nitrogen adsorption analysis. Table 5 summarizes the BET surface area and average pore diameter of the Pd/Ru/Ni (2:8:90)/Al_2O_3 catalyst. Meanwhile, Figures 10 and 11 show the N_2 adsorption–desorption isotherms of the fresh and spent Pd/Ru/Ni (2:8:90)/Al_2O_3 catalysts.

From BET surface area analysis of the Pd/Ru/Ni (2:8:90)/Al_2O_3 catalyst, it can be seen that the surface area of the fresh catalyst was 266.10 m^2g^{-1}; 16.58% higher than its spent catalyst (221.97 m^2 g^{-1}). According to Wan Abu Bakar et al. [36], the BET surface area is presumed to be reduced when there is no generation of new active sites and no transformation of active species occurred during the catalytic reaction. By referring to the EDX analysis, the existence of carbon may also reduce the surface area by blocking the pores of the spent catalyst. As a result, the conversion of CO_2 over the spent Pd/Ru/Ni (2:8:90)/Al_2O_3 catalyst was decreased to 35.10%, compared to the fresh catalyst (43.60%), at the reaction temperature of 200 °C.

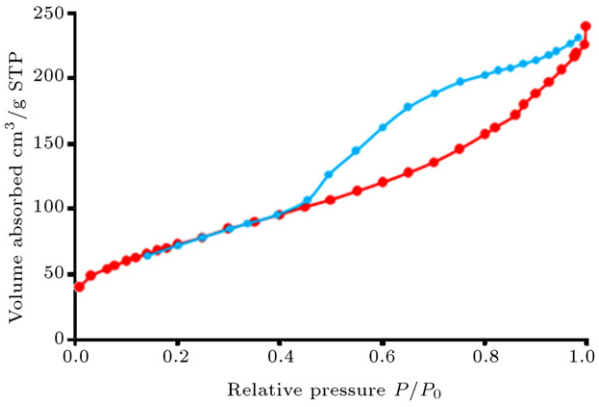

Figure 10: Isotherm plot of fresh Pd/Ru/Ni (2:8:90)/Al_2O_3 catalyst.

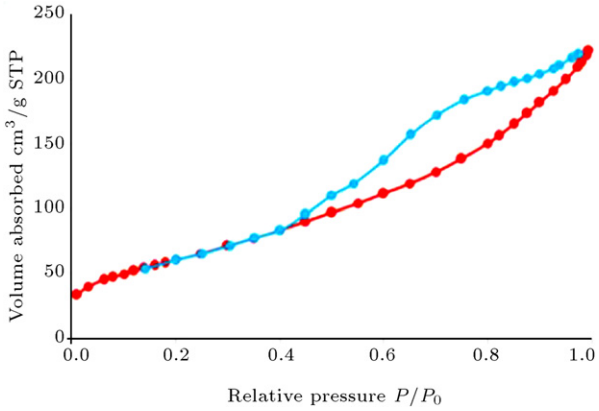

Figure 11: Isotherm plot of spent Pd/Ru/Ni (2:8:90)/Al_2O_3 catalyst.

However, the surface area of the Pd/Ru/Ni (2:8:90)/Al_2O_3 catalyst is considered higher. The higher surface area of the catalyst denoted the increased active sites of the catalyst. This result agrees well with the particle size of the Pd/Ru/Ni (2:8:90)/Al_2O_3 catalyst obtained from the FESEM micrograph, where the catalyst showed nano particle levels. This smaller particle size is presumed to contribute to the increment in surface area. This may contribute to the increasing of catalytic activity over the Pd/Ru/Ni (2:8:90)/Al_2O_3 catalyst, while the average pore diameter of fresh and spent Pd/Ru/Ni (2:8:90)/Al_2O_3 catalysts is around 50 Å. The preferable effect of the pore structure of the support could also enhance the conversion of CO_2, as claimed by Chang et al. [37]. Unfortunately, a nitrogen analysis for the catalyst calcined at 700 and 1000 °C cannot be carried out due to instrument breakdown.

The N_2 adsorption–desorption isotherms of the fresh Pd/Ru/Ni (2:8:90)/Al_2O_3 catalyst demonstrated an isotherm Type IV with a hysteresis loop of type H3 for that of mesoporous materials (Figure 10). The type of isotherm and pore distribution of the Pd/Ru/Ni (2:8:90)/Al_2O_3 catalyst is

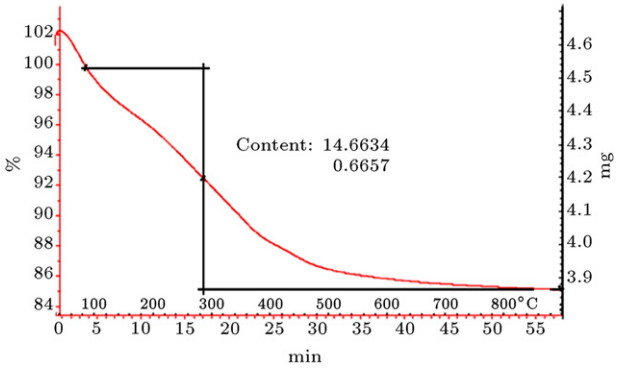

Figure 12: Thermogram of Pd/Ru/Ni (2:8:90)/Al_2O_3 catalyst after aging in an oven for 24 h at 80–90 °C.

similar to the spent catalyst (Figure 11). The mesoporous structure of the nickel oxide catalyst led to an increment in CO_2 performance, which has been mention previously by Inui [2]. The existence of the mesoporous structure gives an optimum pore size in helping to adsorb reactant gases on the surface of the catalyst itself.

3.3.4. Thermogravimetry analysis—differential thermal analysis (TGA-DTA)

After aging the catalysts, which had been prepared by the wetness impregnation method in an oven for 24 h at 80–90 °C, the catalyst was sent for characterization using TGA-DTG. Figure 12 shows the TGA thermogram of the Pd/Ru/Ni (2:8:90)/Al_2O_3 catalyst.

It showed two significant weight lost curves, which occurred around 60 and 280 °C. The total weight loss is 14.66%. Starting from a temperature of 60 °C until 280 °C, free water molecules and the nitrate compound from the supported catalysts were removed, while, 280 °C onwards, the nitrate compound and surface hydroxyl molecule were decomposed from the samples. Savva et al. [38], who studied the Ni/Al_2O_3 catalyst prepared by conventional impregnation and sol–gel methods, found that the physisorbed water was completely removed up to 150 and 200 °C. Meanwhile, the decomposition of nitrate was occurred at a temperature range of 190 °C onwards. Finally, they observed that weight loss at temperatures higher than 360 °C should be attributed to the removal of structural water from the alumina.

From this investigation, the calcination temperature of 400 °C is insufficient to remove all nitrate compounds that originate from the metal precursor. The presence of nitrate compounds in this catalyst was also observed by FTIR analysis, which detected the stretching mode of the free nitrate group. It can be seen that all impurities were removed from the catalysts at temperature higher than 800 °C, meaning that a pure metal oxide had been obtained. Thus, the catalyst calcined at 1000 °C should be good for this catalyst. However, the investigation found that calcination temperatures higher than 400 °C decreased its catalytic activity.

4. Conclusions

The overall performance from catalytic activity studies did not yield any catalyst that gives 100% conversion of CO_2 at lower reaction temperatures. However, Pd/Ru/Ni (2:8:90)/Al_2O_3 was assigned as the most potential catalyst resulted from catalytic activity measurements of FTIR and GC. This catalyst was prepared using the wetness impregnation technique aged at 85 °C, followed by calcination at 400 °C for 5 h. The Pd/Ru/Ni (2:8:90)/Al_2O_3 catalyst shows 43.60% of CO_2 conversion with 6.82% of methane formation at 200 °C. This catalyst had the highest percentage of 52.95% CO_2 conversion, and yielded 39.73% methane at the maximum temperature of 400 °C. In the presence of H_2S in the gas stream, the conversion dropped to 35.03%, with 3.64% yield of methane. However, this catalyst achieved 100% H_2S desulfurization at 140 °C and remained constant until a reaction temperature of 300 °C.

Acknowledgments

The authors gratefully acknowledge the Ministry of Science, Technology and Innovation, Malaysia, for the E-Science Fund Vote 79252, and Universiti Teknologi Malaysia for financial support.

References

[1] Jose, A.R., Jonathan, C.H., Anatoly, I.F., Jae, Y.K. and Manuel, P. "Experimental and theoretical studies on the reaction of H_2 with NiO. Role of O vacancies and mechanism for oxide reduction", *J. Am. Chem. Soc.*, 124, pp. 346–354 (2001).
[2] Inui, T. "Highly effective conversion of carbon dioxide to valuable compounds on composite catalysts", *Catal. Today*, 29, pp. 329–337 (1996).
[3] Souma, Y., Ando, H., Fujiwara, M. and Kieffer, R. "Catalytic hydrogenation of carbon dioxide to hydrocarbons", *Energy Convers. Manage.*, 36(6–9), pp. 593–596 (1995).
[4] Yamasaki, M., Komori, M., Akiyama, E., Habazaki, H., Kawashima, A., Asami, K. and Hashimoto, K. "CO_2 methanation catalysts prepared from amorphous Ni–Zr–Sm and Ni–Zr-misch metal alloy precursors", *Mater. Sci. Eng. A*, 267, pp. 220–226 (1999).
[5] Finch, J.N. and Ripley, D.L. United States Patent 3988334. Retrieved on October 26 (1976) from: http://www.freepatentsonline.com/.
[6] Kusmierz, M. "Kinetic study on carbon dioxide hydrogenation over Ru/γ-Al_2O_3 catalysts", *Catal. Today*, 137, pp. 429–432 (2008).
[7] Takeishi, K. and Aika, K.I. "Comparison of carbon dioxide and carbon monoxide with respect to hydrogenation on Raney ruthenium catalysts", *Appl. Catal. A*, 133, pp. 31–45 (1995).
[8] Miyata, T., Li, D., Shiraga, M., Shishido, T., Oumi, Y., Sano, T. and Takehira, K. "Promoting effect of Rh, Pd and Pt noble metals to the Ni/Mg(Al)O catalysts for the DSS—like operation in CH_4 steam reforming", *Appl. Catal. A*, 310, pp. 97–104 (2006).
[9] Panagiotopolou, P. and Kondarides, D.I. "A comparative study of the water–gas shift activity of Pt catalysts supported on single (MO_x) and composite (MO_x/Al_2O_3, MO_x/TiO_2) metal oxide carriers", *Catal. Today*, 127(1–4), pp. 319–329 (2007).
[10] Erdohelyi, A., Fodor, K. and Szailer, T. "Effect of H_2S on the reaction of methane with carbon dioxide over supported Rh catalysts", *Appl. Catal. B*, 53, pp. 153–160 (2004).
[11] Happel, J. and Hnatow, M.A. United States Patent 4260553. Retrieved on April 7 (1981) from: http://patft.uspto.gov/.
[12] Nurunnabi, M., Muruta, K., Okabe, K., Inaba, M. and Takahara, I. "Performance and characterization of Ru/Al_2O_3 and Ru/SiO_2 catalysts modified with Mn for Fisher–Tropsch synthesis", *Appl. Catal. A*, 340, pp. 203–211 (2008).
[13] Baylet, A., Royer, S., Marecot, P., Tatibouet, J.M. and Duprez, D. "High catalytic activity and stability of Pd doped hexaaluminate catalysts for the CH_4 catalytic combustion", *Appl. Catal. B*, 77, pp. 237–247 (2008).
[14] Bi, Y., Xu, H., Li, W. and Goldbach, A. "Water–gas shift reaction in a Pd membrane reactor over Pt/$Ce_{0.6}Zr_{0.4}O_2$ catalyst", *Int. J. Hydrog. Energy*, 34, pp. 2965–2971 (2009).
[15] Lapisardi, G., Urfels, L., Gelin, P., Primet, M., Kaddouri, A., Garbowski, E., Toppi, S. and Tena, E. "Superior catalytic behaviour of Pt-doped Pd catalysts in the complete oxidation of methane at low temperature", *Catal. Today*, 117, pp. 564–568 (2006).
[16] Gelin, P., Urfels, L., Primet, M. and Tena, E. "Complete oxidation of methane at low temperature over Pt and Pd catalysts for the abatement of lean-burn natural gas fuelled vehicles emissions: influence of water and sulphur containing compounds", *Catal. Today*, 83(1–4), pp. 45–57 (2003).
[17] Yaccato, K., Carhart, R., Hagemeyer, A., Lesik, A., Strasser, P., Volpe, A.F., Turner, H., Weinberg, H., Grasselli, R.K. and Brooks, C. "Competitive CO and CO_2 methanation over supported noble metal catalysts in high throughput scanning mass spectrometer", *Appl. Catal. A*, 296, pp. 30–48 (2005).
[18] Wachs, I.E. "Recent conceptual advances in the catalysis science of mixed metal oxide catalytic materials", *Catal. Today*, 100, pp. 79–94 (2005).
[19] Wu, J.C.S. and Chou, H.C. "Bimetallic Rh-Ni/BN catalyst for methane reforming with CO_2", *Chem. Eng. J.*, 148, pp. 539–545 (2009).

[20] Perkas, N., Amirian, G., Zhong, Z., Teo, J., Gofer, Y. and Gedanken, A. "Methanation of carbon dioxide on Ni catalysts on mesoporous ZrO_2 doped with rare earth oxides", *Catal. Lett.*, 130(3–4), pp. 455–462 (2009).
[21] Ruckenstein, E. and Hu, H.Y. "Carbon dioxide reforming of methane over nickel/alkaline earth metal oxide catalysts", *Appl. Catal. A*, 133, pp. 149–161 (1995).
[22] Takenaka, S., Shimizu, T. and Otsuka, K. "Complete removal of carbon dioxide in hydrogen-rich gas stream through methanation over supported metal catalysts", *Int. J. Hydrog. Energy*, 29, pp. 1065–1073 (2004).
[23] De Boer, M., van Dillen, A.J., Koningsberger, D.C., Geus, J., Vuurman, M.A. and Wachs, I.E. "Remarkable spreading behavior of molybdena on silica catalysts. An in situ EXAFS-Raman study", *Catal. Lett.*, 11, pp. 227–240 (1991).
[24] Habazaki, H., Yamasaki, M., Zhang, B., Kawashima, A., Kohno, S., Takai, T. and Hashimoto, K. "Co-methanation of carbon monoxide and carbon dioxide on supported nickel and cobalt catalysts prepared from amorphous alloy", *Appl. Catal. A*, 172, pp. 131–140 (1998).
[25] Hassan, K.H. "Regeneration and activity test of spent zinc oxide hydrogen sulphide removal catalyst", *Eur. J. Sci. Res.*, 39(2), pp. 289–295 (2010).
[26] Rostrup-Nielsen, J.R. "Chemisorption of hydrogen sulfide on a supported nickel catalyst", *J. Catal.*, 11(3), pp. 220–227 (1968).
[27] Furimsky, E. and Massoth, F.E. "Introduction of regeneration of hydroprocessing catalysts", *Catal. Today*, 17(4), pp. 537–659 (1993).
[28] Trimm, D.L., *Design of Industrial Catalyst*, Elsevier Scientific Publishing Company, The Netherlands, pp. 121–139 (1980).
[29] Silver, R.G., Jackson, N.B. and Ekerdt, J.G. "Adsorption and reaction of carbon dioxide on zirconium dioxide", In *Catalytic Activation of Carbon Dioxide*, W.T. Ayers, Ed., pp. 123–132, American Chemical Society, Washington, DC (1988).
[30] Wang, H.T., Xiao, T.C., Su, J.X., Liu, W.X. and Lu, Y.L. "Catalytic purification of flue gas from civil-used stove", *Catal. Today*, 53, pp. 661–667 (1999).
[31] Chen, X., Zou, H., Chen, S., Dong, X. and Lin, W. "Selective oxidation of CO in excess H_2 over Ru/Al_2O_3 catalyst modified with metal oxide", *J. Nat. Gas Chem.*, 16, pp. 409–414 (2007).
[32] Richardson, J.T., Garrait, M. and Hung, J.-K. "Carbon dioxide reforming with Rh and Pt–Re catalysts dispersed on ceramic foam supports", *Appl. Catal. A*, 255, pp. 69–82 (2003).
[33] Kodama, T., Kitayama, Y., Tsuji, M. and Tamaura, Y. "Methanation of CO_2 using ultrafine $Ni_xFe_{3-x}O_4$", *Energy*, 22(2–3), pp. 183–187 (1997).
[34] Hu, X. and Lu, G. "Inhibition of methane formation in steam reforming reactions through modification of Ni catalyst and the reactants", *Green Chem.*, 11(5), pp. 724–732 (2009).
[35] Paál, Z., Gyorffy, N., Wootsch, A., Tóth, L., Bakos, I., Szabó, S., Wild, U. and Schlögl, R. "Preparation, physical characterization and catalytic properties of unsupported Pt–Rh catalyst", *J. Catal.*, 250(2), pp. 254–263 (2007).
[36] Wan Abu Bakar, W.A., Othman, M.Y., Ali, R., Ching, K.Y. and Toemen, S. "The investigation of active sites on nickel oxide based catalysts towards the in-situ reactions of methanation and desulfurization", *Modern Appl. Sci.*, 3, pp. 35–41 (2009).
[37] Chang, F.W., Hsiao, T.J., Chung, S.W. and Lo, J.J. "Nickel supported on rice husk ash-activity and selectivity in CO_2 methanation", *Appl. Catal. A*, 164, pp. 225–236 (1997).
[38] Savva, P.G., Goundani, K., Vakros, J., Bourikas, K., Fountzoula, C., Vattis, D., Lycourghiotis, A. and Kordulis, C. "Benzene hydrogenation over Ni/Al_2O_3 catalysts prepared by conventional and sol–gel techniques", *Appl. Catal. B*, 79, pp. 199–207 (2008).

Wan Azelee Wan Abu Bakar was born in 1959, in Kelantan, Malaysia. After graduation from the Department of Chemistry at the National University of Malaysia in 1983, he continued his studies into heterogeneous catalysis at Nottingham University, England and received Ph.D. degree in 1995. He then joined Universiti Teknologi Malaysia, where he is currently Professor of Inorganic Chemistry. Professor Wan Azelee Wan Abu Bakar is author of 100 papers published in national and international journals and 4 university chemistry books.

Rusmidah Ali was born in 1957, in Klang, Selangor, Malaysia. She obtained her B.S. degree in Chemistry, in 1980, from Universiti Kebangsaan Malaysia, and her M.S. and Ph.D. degrees from the University of Southampton, England, in 1983 and 1987, respectively. She then joined Universiti Teknologi Malaysia, where she is presently Associate Professor of Inorganic Chemistry. Professor Rusmidah Ali is author of 30 papers published in national and international journals and 11 books.

Susilawati Toemen was born in 1986 in Johor Bahru, Malaysia. She obtained her B.S. and M.S. degrees from Universiti Teknologi Malaysia, in 2008 and 2010, respectively, and is presently studying for her Ph.D. degree at the same institution. She is author of 5 papers published in national and international journals.